Dynamic analysis of chemical eye burns using high-resolution optical coherence tomography

Felix Spöler
Michael Först
Heinrich Kurz
RWTH Aachen University
Institute of Semiconductor Electronics
Sommerfeldstraße 24
52074 Aachen, Germany

Markus Frentz
Norbert F. Schrage
Dept. of Ophthalmology University Aachen
Pauwelsstraße 30
52057 Aachen, Germany
and
Aachen Center of Technology Transfer in Ophthalmology
Karlsburgweg 9
52070 Aachen, Germany

Abstract. The use of high-resolution optical coherence tomography (OCT) to visualize penetration kinetics during the initial phase of chemical eye burns is evaluated. The changes in scattering properties and thickness of rabbit cornea *ex vivo* were monitored after topical application of different corrosives by time-resolved OCT imaging. Eye burn causes changes in the corneal microstructure due to chemical interaction or change in the hydration state as a result of osmotic imbalance. These changes compromise the corneal transparency. The associated increase in light scattering within the cornea is observed with high spatial and temporal resolution. Parameters affecting the severity of pathophysiological damage associated with chemical eye burns like diffusion velocity and depth of penetration are obtained. We demonstrate the potential of high-resolution OCT for the visualization and direct noninvasive measurement of specific interaction of chemicals with the eye. This work opens new horizons in clinical evaluation of chemical eye burns, eye irritation testing, and product testing for chemical and pharmacological products. [DOI: 10.1117/1.2768018]

Keywords: optical coherence tomography (OCT); cornea; eye irritation; eye burns; medical imaging.

Paper 06272SSR received Sep. 29, 2006; revised manuscript received Nov. 30, 2006; accepted for publication Dec. 3, 2006; published online Aug. 2, 2007.

1 Introduction

Optical coherence tomography (OCT) is a noninvasive, noncontact imaging modality that gained great acceptance in ophthalmology as well as in other medical fields due to its high-resolution imaging capability.[1,2] Generating cross-sectional images of tissue morphology at high speed with micrometer scale resolution makes OCT a promising tool for measuring time-dependent physiological and pathophysiological processes in a variety of medical experiments. This technique is especially useful for pharmacological and toxicological studies, which require ongoing monitoring of morphological changes. Here, a promising application of time-resolved OCT imaging is the poorly understood initial phase of chemical eye irritation and interaction of the transparent cornea with corrosives.

OCT imaging of the anterior chamber of the eye was first demonstrated in 1994 by Izatt et al.,[3] admitting noninvasive assessment of the corneal thickness and visualization of the corneal epithelium. A slit-lamp-adapted OCT technique was used to study the cornea after laser thermokeratoplasty and phototherapeutic keratectomy.[4] Abnormal corneal leasons were correlated to slit-lamp biomicroscopy[5] and to histopathology.[6] Ultrahigh-resolution OCT was further demonstrated to be capable of imaging corneal structures like Bowman's and Descement's membrane as well as the typical stromal structure in an animal model[7,8] and in human cornea *postmortem*.[9]

The ability of OCT to gather nondestructively a time series of a single sample with time constants ranging from a split second to long-term observation over several days was utilized for addressing different questions under investigation. For example, wound healing after laser thermal injuring was examined in skin equivalents using OCT and multiphoton microscopy.[10] OCT was used to monitor tissue freezing during cryosurgery,[11] as an *in situ* imaging technique for tissue engineering[12] and to study the heartbeat of small animals.[13,14] In ophthalmology, dynamic OCT measurements were demonstrated to study the corneal response to dehydration stress *in vivo* in a rabbit animal model[15] and to quantify light backscattering within the cornea during corneal swelling.[16]

In chemical eye burns, the validation of the effect of therapeutical intervention by different rinsing solutions in emergency treatment by means of OCT was the objective of the present study. This technique might be helpful to define the action of parameters like temperature, amount, impact force, pH, concentration, redox-potential, and specific reactivity with the ocular tissue that are important for the development of specific treatment procedures.[17] In this article, we evaluate the potential of time-resolved high-resolution OCT imaging to monitor the dynamics of chemical eye burns and the effectiveness of acute intervention procedures in the Ex Vivo Eye Irritation Test (EVEIT). The regions of damaged corneal tissue are characterized with high contrast due to a significant

Address all correspondence to Felix Spöler, RWTH Aachen University, Institute of Semiconductor Electronics, Sommerfeldstrasse 24, 52074 Aachen, Germany. Tel: +49 241 8027896; Fax: +49 241 8022246; E-mail: spoeler@iht.rwth-aachen.de

1083-3668/2007/12(4)/041203/6/$25.00 © 2007 SPIE

increase in light scattering induced by structural changes within the cornea. Our target is to measure speed and characteristics of penetration and propagation as important parameters defining the damage by chemical injury. The direct access to the damaging diffusion process allows for the development of new therapy strategies with reduced number of tests.

2 Materials and Methods

2.1 *OCT System*

The basic principles of OCT are extensively discussed elsewhere.[1,9,18] Briefly, OCT uses the technique of low coherence interferometry, i.e., a light wave is split into a reference beam with variable pathlength and a probe beam, which is focused onto the sample. Backscattered light from inhomogeneities within the sample is recombined with light reflected from the reference arm. An interference signal is generated only if the path difference of both arms is smaller than the coherence length of the light source, thus enabling depth-resolved imaging. For this reason, the axial resolution in OCT is determined by the coherence length of the employed light source. For the high-resolution OCT system employed in this study, a Ti:sapphire laser oscillator (GigaJet 20, GigaOptics GmbH, Konstanz, Germany) centered at 800 nm was used as a low-coherence light source. Additional dispersion management within the laser cavity was deployed to support a spectral bandwidth of 87 nm. The corresponding coherence length was measured to be 3.6 μm in air. The laser output power was 400 mW. The light source was coupled in the fiber-based interferometer of a commercially available OCT system (Sirius 713, Heidelberg Engineering GmbH, Lübeck, Germany).[19] The latter was modified to support the superior axial resolution specified by the coherence length of the Ti:sapphire oscillator. A flexible applicator was employed[19] to allow for horizontal positioning of the corneal surface under investigation. The A-scan rate was 50 Hz, and the number of data points for each A-line data acquisition was 512. The imaging depth was 845 μm in air (610 μm in tissue), and the focal position of the imaging beam within tissue was approximately 400 μm below the upper border of the image. The sample arm power was 3 mW, and the axial and lateral resolutions were 3 and 8 μm, respectively.

2.2 *Ex Vivo Eye Irritation Test (EVEIT)*

Experiments were performed using the EVEIT. This model has been proven to react very similar to living eye tissue concerning the behavior during a chemical eye burn.[20] In this study, enucleated white rabbit eyes were used. Rabbit heads were obtained from abattoir and kept cool until enucleation of the eyes. The globes were stored at 4 °C in a humid atmosphere to ensure preservation of the corneal epithelium. Only clear corneas without any epithelial defects were processed. All measurements were performed within 12 h after animal death.

2.3 *Measurement*

OCT images were composed of up to 1000 A-scans with a lateral step size of 6 μm for static tissue examination. Images with a width of 600 μm (100 A-scans per image) were taken at a rate of 30 frames per min for time-resolved measurements.

OCT measurements were performed at the center of the cornea. Care was taken to ensure orthogonality of the sample beam to the surface of the probe for the measurements of central corneal thickness and central epithelial thickness. Minor tipping of the probe was used to eliminate the central corneal reflex in the tomograms presented in this study. For comparison, the cornea of each eye was imaged directly before application of the chemicals. Chemical injury was induced by superficial exposure of the cornea to the chemical under investigation. The application of a standardized amount was ensured by spraying 500 μl of the chemical by an Eppendorf pipette onto the center of the cornea, which was positioned horizontally. By this means, a continuous film of the fluid is spread over the cornea, thinning out with time. This development is directly monitored in OCT imaging. Penetration of the chemical within the cornea was imaged starting directly after its application. A refractive index of 1.385 was used for the conversion of optical to geometrical path lengths measured by OCT.[21] It was further assumed that the index of refraction does not significantly change during chemical burn.

Evaluation of the effectiveness of rinsing as first aid treatment was accomplished by comparing OCT images of rinsed and untreated burned eyes at the same time-steps after application of the chemical. Both eyes used in one experiment were obtained from the same animal for direct comparability. One eye was not treated after application of the corrosive. The other eye was rinsed for 15 min starting 20 s after application of the chemical onto the cornea. An infusion system with a flow rate of 67 ml/min was used for this purpose. Tomograms of both eyes obtained 16 min after exposure to the corrosive were compared in order to evaluate the effect of the rinsing solution.

The chemicals applied were 0.5, 1, and 2 molar NaOH as well as 1 molar H_2SO_4. For rinsing, we used 1000 ml of Previn solution (Prevor, Inc.), which is recommended as an amphoteric therapeutical solution in any type of severe eye burns. The activity of this solution was described earlier.[22]

The color scale of the OCT images represents the intensity only and contains no spectral information (color online only). The same logarithmic color scale as given in the inset of Fig. 1(b) is used for all OCT images, and the same intensity scale was used for all A-scans.

3 Results

A characteristic high-resolution image of an untreated rabbit cornea *ex vivo* is shown in Fig. 1(a). The magnification of the central section of the cornea is given in Fig. 1(b). Here, the epithelial and endothelial layers, the stroma, and allusively, the stromal fibers are distinguishable. The Descement's membrane separating the stroma from the endothelium is imaged as low scattering band, which is clearly silhouetted against the higher scattering surrounding layers. Ten adjacent A-scans around the center of the image were averaged to determine layer thicknesses [Fig. 1(c)]. Here, the boundaries of the different layers are illustrated by peaks in signal intensity with high contrast, whereas the Descement's membrane is represented by a noticeable drop of the OCT signal.

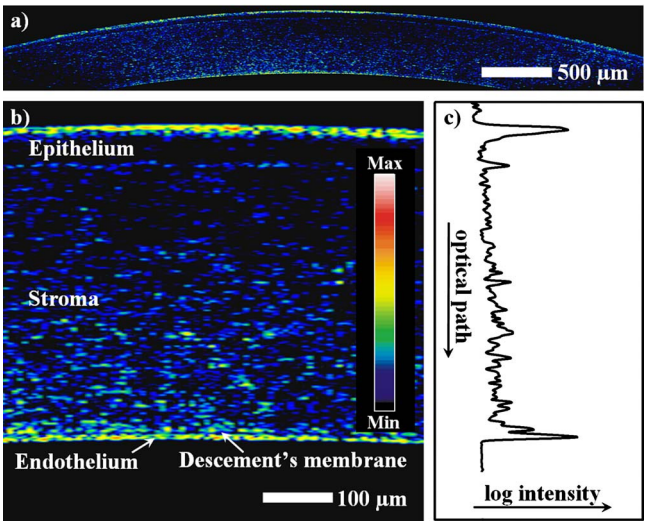

Fig. 1 High-resolution OCT image of an untreated rabbit cornea *ex vivo*. (a) Overview over the scanned region, 4.5 mm in width. (b) Magnification of the central section (600 μm × 600 μm) of the cornea. The logarithmic color scale used for all OCT images within this study is given in the inset of this figure (color online only). (c) Intensity profile corresponding to (b) given by the average of ten adjacent A-scans.

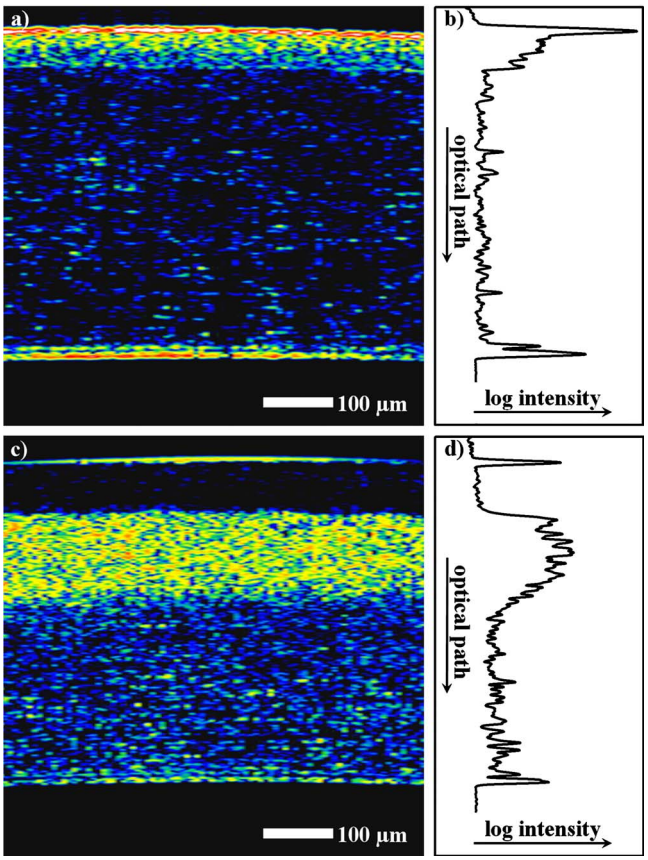

Fig. 2 Tomographic images (600 μm × 600 μm) and corresponding A-scans of corneal tissue damage caused by topical application of corrosives. (a) Section 10 min after topical application of a 1 molar solution of 500 μl H_2SO_4. (b) Intensity profile corresponding to (a) given by the average of ten adjacent A-scans. (c) Section 10 min after topical application of a 0.5 molar solution of 500 μl NaOH. (d) Intensity profile corresponding to (c) given by the average of ten adjacent A-scans.

For direct comparison, OCT images of corneal tissue damage caused by chemical interaction are presented in Fig. 2. Tomograms taken 10 min after topical application of a 1 molar solutions of sulfuric acid (H_2SO_4) and a 0.5 molar solution of sodium hydroxide (NaOH) are shown in Figs. 2(a) and 2(c), respectively. Corresponding diagrams of 10 averaged A-scans are depicted in Figs. 2(b) and 2(d). Tissue damage is delineated with high contrast indicated by a significant increase in OCT signal intensity compared to the image taken prior to the application of the chemical (Fig. 1). The microstructure of the stromal fibers, which is oriented strictly parallel to the corneal surface in unburned eyes, changes to a structure without specific orientation after interaction with the alkaline solution.

For the case of H_2SO_4 application, an increase in signal amplitude is restricted to the epithelial layer, while structure and thickness of the stroma appear unchanged. However, penetration of sulfuric acid within the upper part of the stroma was observed for concentrations of 2 mol/l. With the exception of hydrofluoric acid, the tendency to remain on the ocular surface was also observed for other acids of moderate concentration, e.g., hydrochloric acid (not shown here).

In contrast, after NaOH application, the inner structure of the epidermal layer appears almost unchanged in OCT imaging, while its thickness increases by a factor of 1.5. Significant increase in light scattering within the stroma was found even for low concentrations of NaOH. Other alkalis like calcium hydroxide were found to react similarly (not shown here). The easy and fast penetration of alkalis throughout the cornea and the anterior segment is the central issue of the severe clinical manifestation of the alkali-injured eye.

To gain insight into the dynamics of the extensive tissue damage observed for alkali-induced eye burns, OCT image sequences applied after superficial exposure of the cornea to a 1 molar and a 2 molar solution of NaOH are compared in Fig. 3. The corresponding cross-sectional image of the cornea before NaOH application is given in the leftmost image. Time-steps given within the following pictures refer to zero time delay ($t=0$), when the NaOH is applied onto the corneal surface. The liquid film of the applied alkaline solution is imaged in the subsequent tomograms. It is distinguishable from the epithelium by the absence of internal scattering. A decrease of the film thickness of the NaOH solution in combination with swelling of the epithelium is observed over time. Penetration of the corrosive within the stroma is indicated by an increase in signal amplitude for affected areas. Full penetration of the cornea is completed within 120 s for 1 molar NaOH and within 38 s for 2 molar NaOH. The temporal evolution of the penetration depth was obtained from averaged A-scans of the OCT image sequence given in Fig. 3. Here it was assumed that the front of penetration is given by the significant drop of scattering intensity within the stroma. The penetration velocity was found to increase with concentration and to exponentially decrease with time of penetration (Fig. 4). For NaOH concentrations of 0.5 mol/l, the penetration velocity falls down to zero within the cornea and there-

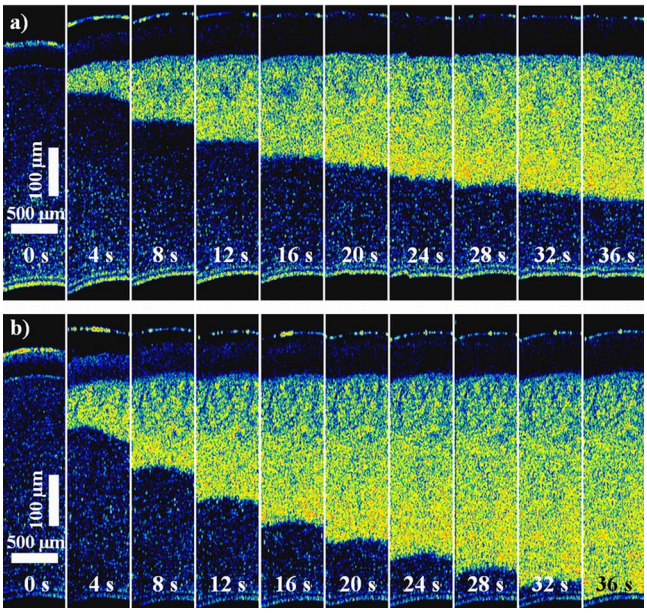

Fig. 3 OCT image sequences illustrating corneal tissue damage caused by topical application of 500 μl of differently concentrated NaOH. (a) 1 molar solution; (b) 2 molar solution.

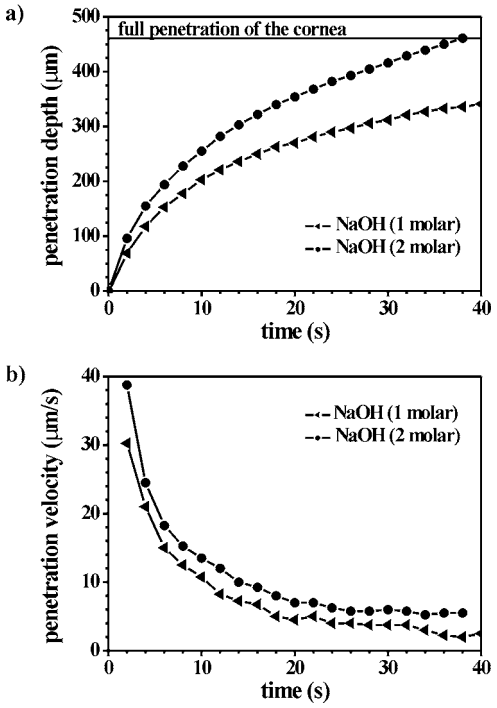

Fig. 4 Numeric analysis of NaOH penetration time and velocity within rabbit cornea derived from OCT time series. (a) Plot of penetration depth of NaOH (1 and 2 molar solutions) versus time after topical application. (b) Plot of the penetration velocity of NaOH solutions versus time after topical application given by the derivative of plot (a).

fore full penetration of the cornea was not observed. No discontinuity of the penetration could be found for the transition from epithelium to stroma.

The capability of OCT to monitor the effectiveness of rinsing as first aid treatment for chemical eye burns is demonstrated in Fig. 5. Figure 5(a) shows an unrinsed burned eye, while the rabbit eye imaged in Fig. 5(b) was rinsed for 15 min starting 20 s after application of the corrosive using 1000 ml of Previn solution (Prevor, Inc.). Both eyes were imaged 16 min after chemical eye burn with 1 M NaOH. There is clear evidence in Fig. 5(a) that without rinsing, a large scattering amplitude is observed over the complete cross-sectional area of the stroma, which indicates full corneal penetration of the corrosive. In contrast, the lower half of the stroma appears almost unchanged in the OCT image for the rinsed eye. Additionally, after alkali eye burn and subsequent rinsing, the epithelial layer has disappeared.

4 Discussion

In this study, we demonstrate the benefits of high-resolution OCT imaging for providing objective information about the pathophysiological damage caused by chemical eye burns in an *ex vivo* animal model. A primary source of contrast in OCT is the local scattering cross section. Injury of the eye initiated by a corrosive changes inherently the scattering properties of the tissue. This process can be effectively monitored with high spatial and temporal resolution using OCT imaging. Using high-resolution OCT, additional information about the resistance of potential barriers like the Descement's membrane as well as microstructural changes as observed for the orientation of the stromal fibers can be extracted.

The inner structure of a healthy rabbit cornea *ex vivo* is illustrated by high-resolution OCT (Fig. 1). Here, the cellular and lamellar structure is accessible. The cross-sectional information is comparable to slit-lamp microscopy, with improved detection of inner corneal layers including Descemet's membrane and endothelium. The central epithelial thickness was measured to be 47 μm on the average, which is in close agreement to the value of 45.8 μm given by Reiser et al.[8] for the same *ex vivo* animal model. The averaged central corneal thickness (CCT) derived from recorded OCT images was 445 μm with a standard deviation of 21 μm. This value is significantly larger than the CCT of approximately 360 μm measured by pachymetry for *in vivo* rabbit eyes.[23] Slight overhydration causing an increase of corneal thickness is known to be due to the 4 °C storage and consecutive low pumping activity of the endothelium.

The microstructure of the tissue under investigation determines its scattering cross section and therefore the OCT signal amplitude. In reverse, the change of tissue appearance in OCT images caused by interaction with a corrosive can be ascribed to structural changes caused by the chemical. Healthy corneal stroma transmits 99% of the incident light without scattering.[24] It is generally accepted that the fibril diameter, the interfibrillar distance, and the lattice-like organization of the collagen fibrils play a crucial role in stromal transparency.[25] Any structural changes within the stroma will result in corneal opacification. For chemical eye burns, structural disorders are initiated by direct chemical interaction as well as by water-electrolyte imbalance followed by a change of the hydration state within the stroma.[26] These structural changes can be observed by OCT for alkalis [Figs. 2(b) and 3] as well as for acids that penetrate within the stroma.

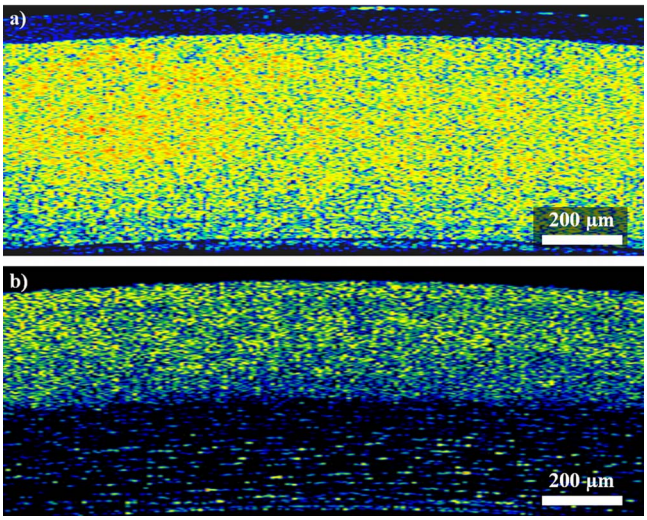

Fig. 5 Demonstration of the effectiveness of rinsing as a first aid treatment after chemical eye burn. Two rabbit corneas were imaged 16 min after topical application of a 1 molar solution of 500 μl NaOH. (a) No intervention procedure has been carried out between application of the chemical and OCT imaging. (b) The eye was rinsed with 1000 ml Previn for 15 min starting 20 s after application of the NaOH solution.

In corneal damage caused by acids, the anion involved, i.e., SO_4^{2-} for the case of sulfuric acid, gives rise to protein denaturation and subsequent opacification of the epithelium,[26] as is observed in Fig. 2(a). The acid-induced coagulation of proteins within the epithelium acts as a barrier for further penetration.[26] Therefore, the appearance of the stroma typically remains constant after application of moderately concentrated acids onto the eye [Fig. 2(a)].

Alkalis penetrate very rapidly into the eye. In the epithelium, the structural dissolution of cell membranes by saponification in alkali can be detected by the low reflection within this layer [see Fig. 2(b)]. The total loss of integrity of the epithelium is confirmed by OCT imaging after rinsing [Fig. 5(b)]. Here, the epithelium has vanished as the cellular fragments are washed away by the solvent. Histological examination after corneal NaOH burn also demonstrate the loss of this cellular layer.[27]

Alkali-induced structural breakdown of the corneal matrix is a well-known fact shown by the experiments of Pfister et al., who exposed healthy tissues with proteins collected from freshly burnt corneas.[28] Structural damage within the stroma is induced by the cation of the alkali, which reacts with the carboxyl groups of stromal collagen and glycosaminoglycans.[26] Such direct chemical interaction does not take place if the cornea is exposed to a neutral hyperosmolar rinsing solution like Previn solution (Prevor, Inc.). OCT imaging during treatment of unburned eyes with this solution shows shrinkage of the corneal thickness as well as an associated minor increase in OCT signal amplitude. The same effect is observed for the lower part of the stroma after rinsing a burned eye [Fig. 5(b)]. This observation can be contributed to the dehydration of the cornea through the semipermeable corneal epithelium.[29] Here, the observed increase in scattering induced by the change in the hydration state of the stroma is marginal compared to that observed after application of a corrosive. This indicates that structural damage by direct chemical interaction with the corrosive induces the observed distinct increase in OCT signal during chemical eye burn. Further evidence to this hypothesis is given by comparing direct measurements of alkali penetration time to the time-resolved OCT data. Topical application of 2 molar NaOH results in a rise of the intracameral pH value after a delay of approximately 50 s.[22] This measurement of the penetration time throughout the cornea corresponds well to the value of 38 s derived from OCT imaging as given in Fig. 4(a). As the pH electrode in intracameral pH measurement is not placed directly at the endothelium of the cornea, the observed discrepancy in full corneal penetration time compared to the time derived from OCT measurements can be ascribed to the diffusion time of the corrosive within the aqueous humor. For this reason, the direct measurement of the diffusion time is comparable to the time-resolved OCT experiments introduced in this study. This verifies that the increase in scattering cross section within the stroma is an instantaneous process on the time scale under consideration and therefore is a useful measure to determine the depth of penetration of the corrosive. Using time-resolved OCT imaging to examine chemical eye burns, additional parameters not accessible by established methods, e.g., intracameral pH measurement, can be derived within the present study. Spatial resolution provided by OCT gives access to investigate the depth-dependent penetration velocity [see Fig. 4(b)]. For NaOH application, the penetration velocity was observed to decrease with penetration depth. For 2 molar NaOH the diffusion velocity decreases from about 40 μm/s to 5 μm/s during corneal penetration. For a NaOH concentration of 1 mol/l, the diffusion velocity is reduced below 1 μm/s at the bottom part of the stroma. Besides the consumption of the reactants, which undergo chemical reactions, dilution of the corrosive within the tissue might play a role for this deceleration. This is consistent with the strong correlation of penetration velocity on the concentration of the applied NaOH solution [Fig. 4(b)].

As demonstrated in Figs. 2 and 3, OCT imaging allows for observation of chemical eye burns before full corneal penetration is reached. From the time measured for half cornea penetration, conclusions can be drawn about the time frame that is available for effective intervention procedures like rinsing. Immediate rinsing of the eye is the most important factor in emergency treatment of chemical eye burns. The recommended therapeutic solutions differ with type of chemical reaction and buffer capacity. Here, only few data on the comparative application of rinsing solutions exist.[22] OCT is able to supply objective information about the effectiveness of rinsing therapy, e.g., prevention of structural changes and precipitation within the corneal stroma induced by the rinsing solution. The latter negative effect was observed using phosphate buffer as rinsing solution.[30,31] Comparison of the appearance of chemical eye burns induced by 1 molar NaOH without rinsing and after rinsing using a commercial antidote for chemical burns demonstrates the potential of this imaging technique for the quantification of first aid treatment conditions (Fig. 5). The status after rinsing can be compared directly to the status at that time-step where rinsing was started [given by the time series data set in Fig. 3(a)]. When rinsing

was started 20 s after NaOH application, the stroma was halfway penetrated by the alkali. In the example introduced here, this status was preserved under the described rinsing conditions by effectively inhibiting further penetration. Furthermore, no structural changes of the intact part of the tissue due to exposure to the rinsing solution was observable using OCT.

In summary, we showed that high-resolution OCT is capable of imaging the dynamics of chemical eye burns in real time. It was demonstrated that OCT is sensitive to the change in the optical properties of the cornea, which can be correlated to changes in the microstructure as a result of chemical damage. Here, the advantage of OCT compared to standard methods like histopathology and measurement of the intracameral pH is the extent of information that can be achieved by time-resolved OCT imaging of corneal penetration. OCT as an instrument for high-contrast imaging of chemical eye burns might lead to further insight into the mechanism of this kind of injuries. Due to the possibility for noninvasive serial measurements, OCT should be employed as a valuable tool in the diagnosis of eye irritation as well as in detection of biological and structural chemical changes, giving objective measures for quantifying the effect of rinsing solutions. This system accomplishes the EVEIT research in chemical product testing, replacing research on living animals, e.g., within the REACH-System (Registration, Evaluation, and Authorization of Chemicals), a new regulatory framework in the European Union.

References

1. D. Huang, E. A. Swanson, C. P. Lin, J. S. Schuman, W. G. Stinson, W. Chang, M. R. Hee, T. Flotte, K. Gregory, C. A. Puliafito, and J. G. Fujimoto, "Optical coherence tomography," *Science* **254**, 1178–1181 (1991).
2. J. G. Fujimoto, "Optical coherence tomography for ultrahigh resolution *in vivo* imaging," *Nat. Biotechnol.* **21**, 1361–1367 (2003).
3. J. A. Izatt, M. R. Hee, E. A. Swanson, C. P. Lin, D. Huang, J. S. Schuman, C. A. Puliafito, and J. G. Fujimoto, "Micrometer-scale resolution imaging of the anterior eye *in vivo* with optical coherence tomography," *Arch. Ophthalmol. (Chicago)* **112**, 1584–1589 (1994).
4. H. Hoerauf, C. Wirbelauer, C. Scholz, R. Engelhardt, P. Koch, H. Laqua, and R. Birngruber, "Slit-lamp-adapted optical coherence tomography of the anterior segment," *Graefe's Arch. Clin. Exp. Ophthalmol.* **238**, 8–18 (2000).
5. K. Hirano, Y. Ito, T. Suzuki, T. Kojima, S. Kachi, and Y. Miyake, "Optical coherence tomography for the noninvasive evaluation of the cornea," *Cornea* **20**, 281–289 (2001).
6. C. Wirbelauer, J. Winkler, G. O. Bastian, H. Häberle, and D. T. Pham, "Histopathological correlation of corneal diseases with optical coherence tomography," *Graefe's Arch. Clin. Exp. Ophthalmol.* **240**, 727–734 (2002).
7. K. Grieve, M. Paques, A. Dubois, J. Sahel, C. Boccara, and J.-F. L. Gargasson, "Ocular tissue imaging using ultrahigh-resolution full-field optical coherence tomography," *Invest. Ophthalmol. Visual Sci.* **45**, 4126–4131 (2004).
8. B. J. Reiser, T. S. Ignacio, Y. Wang, M. Taban, J. M. Graff, P. Sweet, Z. Chen, and R. S. Chuck, "*In vitro* measurement of rabbit corneal epithelial thickness using ultrahigh resolution optical coherence tomography," *Vet. Ophthalmol.* **8**, 85–88 (2005).
9. W. Drexler, "Ultrahigh-resolution optical coherence tomography," *J. Biomed. Opt.* **9**, 47–74 (2004).
10. A. T. Yeh, B. Kao, W. G. Jung, Z. Chen, J. S. Nelson, and B. J. Tromberg, "Imaging wound healing using optical coherence tomography and multiphoton microscopy in an *in vitro* skin-equivalent tissue model," *J. Biomed. Opt.* **9**, 248–253 (2004).
11. B. Choi, T. E. Milner, J. Kim, J. N. Goodman, G. Vargas, G. Aguilar, and J. S. Nelson, "Use of optical coherence tomography to monitor biological tissue freezing during cryosurgery," *J. Biomed. Opt.* **9**, 282–286 (2004).
12. C. Mason, J. F. Markusen, M. A. Town, P. Dunnill, and R. K. Wang, "The potential of optical coherence tomography in the engineering of living tissue," *Phys. Med. Biol.* **49**, 1097–1115 (2004).
13. S. A. Boppart, G. J. Tearney, B. E. Bouma, J. F. Southern, M. E. Brezinski, and J. G. Fujimoto, "Noninvasive assessment of the developing xenopus cardiovascular system using optical coherence tomography," *Proc. Natl. Acad. Sci. U.S.A.* **94**, 4256–4261 (1997).
14. M. A. Choma, S. D. Izatt, R. J. Wessells, R. Bodmer, and J. A. Izatt, "Images in cardiovascular medicine: *In vivo* imaging of the adult drosophila melanogaster heart with real-time optical coherence tomography," *Circulation* **114**, e35–e36 (2006).
15. K. Hosseini, A. I. Kholodnykh, I. Y. Petrova, R. O. Esenaliev, F. Hendrikse, and M. Motamedi, "Monitoring of rabbit cornea response to dehydration stress by optical coherence tomography," *Invest. Ophthalmol. Visual Sci.* **45**, 2555–2562 (2004).
16. J. Wang, T. L. Simpson, and D. Fonn, "Objective measurements of corneal light-backscatter during corneal swelling, by optical coherence tomography," *Invest. Ophthalmol. Visual Sci.* **45**, 3493–3498 (2004).
17. N. F. Schrage, S. Langefeld, J. Zschocke, R. Kuckelkorn, C. Redbrake, and M. Reim, "Eye burns: An emergency and continuing problem," *Burns* **26**, 689–699 (2000).
18. A. F. Fercher, W. Drexler, C. K. Hitzenberger, and T. Lasser, "Optical coherence tomography—principles and applications," *Rep. Prog. Phys.* **66**, 239–303 (2003).
19. J. Welzel, "Optical coherence tomography in dermatology: A review," *Skin Res. Technol.* **7**, 1–9 (2001).
20. S. Kompa, B. Schareck, J. Tympner, H. Wüstemeyer, and N. F. Schrage, "Comparison of emergency eye-wash products in burned porcine eyes," *Graefe's Arch. Clin. Exp. Ophthalmol.* **240**, 308–313 (2002).
21. W. Drexler, C. K. Hitzenberger, A. Baumgartner, O. Findl, H. Sattmann, and A. F. Fercher, "Investigation of dispersion effects in ocular media by multiple wavelength partial coherence interferometry," *Exp. Eye Res.* **66**, 25–33 (1998).
22. S. Rihawi, M. Frentz, and N. F. Schrage, "Emergency treatment of eye burns: Which rinsing solution should we choose?" *Graefe's Arch. Clin. Exp. Ophthalmol.* **244**, 845–854 (2006).
23. S. Kompa, E. Ehlert, M. Reim, and N. F. Schrage, "Microbiopsy in healthy rabbit corneas: A long-term study," *Acta Ophthalmol. Scand.* **78**, 411–415 (2000).
24. K. M. Meek and D. W. Leonard, "Ultrastructure of the corneal stroma: A comparative study," *Biophys. J.* **64**, 273–280 (1993).
25. R. W. Hart and R. A. Farrell, "Light scattering in the cornea," *J. Opt. Soc. Am.* **59**, 766–774 (1969).
26. M. D. Wagoner, "Chemical injuries of the eye: Current concepts in pathophysiology and therapy," *Surv. Ophthalmol.* **41**, 275–313 (1997).
27. J. Čejková, Z. Lojda, E.-M. Salonen, and A. Vaheri, "Histochemical study of alkali-burned rabbit anterior eye segment in which severe lesions were prevented by aprotinin treatment," *Histochemistry* **92**, 441–448 (1989).
28. R. R. Pfister and J. L. Haddox, "A neutrophil chemoattractant is released from cellular and extracellular components of the alkali-degraded cornea and blood," *Invest. Ophthalmol. Visual Sci.* **37**, 230–237 (1996).
29. S. Kompa, C. Redbrake, C. Hilgers, H. Wüstemeyer, N. Schrage, and A. Remky, "Effect of different irrigating solutions on aqueous humour pH changes, intraocular pressure and histological findings after induced alkali burns," *Acta Ophthalmol. Scand.* **83**, 467–470 (2005).
30. N. F. Schrage, B. Schlossmacher, W. Aschenbernner, and S. Langefeld, "Phosphate buffer in alkali eye burns as an inducer of experimental corneal calcification," *Burns* **27**, 459–464 (2001).
31. W. Bernauer, M. A. Thiel, M. Kurrer, A. Heiligenhaus, K. M. Rentsch, A. Schmitt, C. Heinz, and A. Yanar, "Corneal calcification following intensified treatment with sodium hyaluronate artificial tears," *Br. J. Ophthamol.* **90**, 285–288 (2006).